REPORT DOCUMENTATION PAGE

Form Approved
OMB No. 0704-0188

1. REPORT DATE *(DD-MM-YYYY)*	**2. REPORT TYPE**	**3. DATES COVERED** *(From - To)*
23-06-2008	Technical Paper	

4. TITLE AND SUBTITLE

Effect of Anode Current Fluctuations on Ion Energy Distributions within a 600 W Hall Effect Thruster (Preprint)

5a. CONTRACT NUMBER

5b. GRANT NUMBER

5c. PROGRAM ELEMENT NUMBER

6. AUTHOR(S)
William A. Hargus, Jr. (AFRL/RZSS); Michael R. Nakles (ERC); Rachel Tedrake, Bruce Pote (Busek)

5d. PROJECT NUMBER

5e. TASK NUMBER

5f. WORK UNIT NUMBER
33SP0706

7. PERFORMING ORGANIZATION NAME(S) AND ADDRESS(ES)

Air Force Research Laboratory (AFMC)
AFRL/RZSS
1 Ara Drive
Edwards AFB CA 93524-7013

8. PERFORMING ORGANIZATION REPORT NUMBER

AFRL-RZ-ED-TP-2008-244

9. SPONSORING / MONITORING AGENCY NAME(S) AND ADDRESS(ES)

Air Force Research Laboratory (AFMC)
AFRL/RZS
5 Pollux Drive
Edwards AFB CA 93524-7048

10. SPONSOR/MONITOR'S ACRONYM(S)

11. SPONSOR/MONITOR'S NUMBER(S)
AFRL-RZ-ED-TP-2008-244

12. DISTRIBUTION / AVAILABILITY STATEMENT

Approved for public release; distribution unlimited (PA #08255A).

13. SUPPLEMENTARY NOTES
For presentation at the 44th AIAA Joint Propulsion Conference, Hartford, CT, 20-23 July 2008.

14. ABSTRACT

This work presents axial ion energy distribution measurements within the acceleration channel of the 600 W Busek Co. Inc. BHT-HD-600 laboratory Hall thruster derived from laser-induced fluorescence measurements of the $5d[4]_{7/2} - 6p[3]_{5/2}$ xenon ion excited state transition. Acceleration channel centerline ion energy distributions are measured for three closely related operating conditions which only differ in the magnitude of the radial magnetic field strength. These three operating conditions span a broad range of discharge current oscillations strength. The 0 to 200 kHz frequency domain is characterized, and the dominant 40 kHz to 50 kHz frequency appears most likely to be axially traveling ionization waves, commonly known as the *breathing mode oscillations*. These oscillations manifest themselves to the laser induced fluorescence diagnostic as clearly broadened ion energy distributions when the oscillation strength is high. We determine the spatial extent of the axial breathing mode oscillation nonintrusively. The coherence and magnitude of the discharge current oscillations are inversely proportional to acceleration channel radial magnetic strength.

15. SUBJECT TERMS

16. SECURITY CLASSIFICATION OF:			**17. LIMITATION OF ABSTRACT**	**18. NUMBER OF PAGES**	**19a. NAME OF RESPONSIBLE PERSON**
					Dr. William A. Hargus, Jr.
a. REPORT	**b. ABSTRACT**	**c. THIS PAGE**	SAR	11	**19b. TELEPHONE NUMBER** *(include area code)*
Unclassified	**Unclassified**	**Unclassified**			N/A

Effect of Anode Current Fluctuations on Ion Energy Distributions within a 600 W Hall Effect Thruster (Preprint)

William A. Hargus, Jr.*
Michael R. Nakles†
Spacecraft Propulsion Branch
Air Force Research Laboratory
Edwards AFB, CA 93524

Rachel Tedrake‡
Bruce Pote§
Electric Propulsion Group
Busek Company, Inc.
Natick, MA 01760

This work presents axial ion energy distribution measurements within the acceleration channel of the 600 W Busek Co. Inc. BHT-HD-600 laboratory Hall thruster derived from laser-induced fluorescence measurements of the $5d[4]_{7/2} - 6p[3]_{5/2}$ xenon ion excited state transition. Acceleration channel centerline ion energy distributions are measured for three closely related operating conditions which only differ in the magnitude of the radial magnetic field strength. These three operating conditions span a broad range of discharge current oscillations strengths. The 0 to 200 kHz frequency domain is characterized, and the dominant 40 kHz to 50 kHz frequency appears most likely to be axially traveling ionization waves, commonly known as the *breathing mode oscillations.* These oscillations manifest themselves to the laser induced fluorescence diagnostic as clearly broadened ion energy distributions when the oscillation strength is high. We determine the spatial extent of the axial breathing mode oscillation nonintrusively. The coherence and magnitude of the discharge current oscillations are inversely proportional to acceleration channel radial magnetic strength.

Introduction

The goal of this study is to characterize the xenon ion energy distributions inside the acceleration channel of a low power xenon Hall thruster using laser-induced fluorescence (LIF) and assess the effect of discharge plasma oscillations on the distribution of ion energies. Although the discharge of a Hall thruster appears to be a quiescent plasma, it can be a highly oscillatory plasma with a variety of axial, azimuthal, and possibly radial modes. Understanding these oscillations is necessary to the application and interpretation of the any internal measurements for thruster plasma model validation.

Ion velocity and energy distribution measurements are valuable for their use in the validation of device models of this and other Hall thrusters as they provide a direct comparison of measurement to simulation results. Previous attempts to compare bulk ion velocities from experiments with results of numerical simulations have encountered difficulties. For example, simulation efforts usually report mean velocities. Experimental methods such LIF are often noise limited and are better suited to determining the most probable velocity. In the skewed, non-symmetric velocity distributions common to Hall thrusters, the most probable (i.e. peak signal) and statistical mean velocities often differ. Ideally, comparison of the velocity distribution function determined from each method would minimize ambiguity. Due to the relatively narrow transition width and wide velocity distribution, these fluorescence traces have been previously shown to be representative of the ion velocity distribution function and can also be used to calculate ion energy distributions.[1]

American Institute of Aeronautics and Astronautics
Approved for public release; distribution is unlimited.

Most previous internal measurements of ion velocities and energies have been carried out using a slot cut into the side of a Hall thrusters.[2,3] These slots presumably affect the operation of the thruster. Even if the global effect is small, the local effect may be significant. Furthermore, slicing slots into Hall thruster side walls is not always possible with expensive, one of kind, test articles.

Most modern Hall thrusters have acceleration channels with a maximum depth of 1-2 cm. Therefore, it is possible to align collection optics to the probe beam such that limited internal optical access is possible without modification of the Hall thruster. In this work, the collection lens is placed 60° off the plume axis. This minimizes plume impact since typically greater than 95% of a Hall thruster plume ion flux is contained in a 45° half angle. In this way, it is possible to completely non-intrusively probe internal ion acceleration of any modern Hall thruster[4]

In this study acceleration channel centerline ion energy distributions are measured for three closely related operating conditions which only differ in the magnitude of the radial magnetic field strength. These three operating conditions span a broad range of discharge current oscillations strengths from mild broad band oscillations at the highest radial magnetic field strength to highly coherent oscillations which dominate the discharge current at the lowest magnetic field strength.

Experimental Apparatus

Xenon Ion Spectroscopy

LIF is a convenient diagnostic for the investigation of ion and atomic velocities as it does not perturb the plasma. The LIF signal is a convolution of the velocity distribution, transition line shape, and laser beam frequency profile. Determination of the velocity distribution from LIF data only requires the deconvolution of the transition line shape and laser beam profile from the raw LIF signal trace. Subsequently, it is straightforward to calculated the energy distribution from the the velocity distribution.

For the results reported here, the $5d[4]_{7/2}-6p[3]_{5/2}$ electronic transition of Xe II at 834.7 nm is probed. The isotopic and nuclear-spin effects contributing to the hyperfine structure of the $5d[4]_{7/2} - 6p[3]_{5/2}$ xenon ion transition produce a total of 19 isotopic and spin split components. The hyperfine splitting constants which characterize the variations in state energies are only known for a limited set of energy levels. Unfortunately, the 834.7 nm xenon ion transition only has confirmed data on the nuclear spin splitting constants of the $6p[3]_{5/2}$ upper state.[2,5–7] Manzella first used the $5d[4]_{7/2} - 6p[3]_{5/2}$ xenon ion transition at 834.7 nm to make velocity measurements in a Hall thruster plume.[8] A convenient feature of this transition is the presence of a relatively strong line originating from the same upper state ($6s[2]_{3/2} - 6p[3]_{5/2}$ transition at 541.9 nm,[9] which allows for non-resonant fluorescence collection). Ion velocity is simply determined by measurement of the Doppler shift of the absorbing ions.[10]

Previous measurements and analysis have shown that deconvolution is not strictly required to estimate xenon ion velocity and energy distributions from the raw LIF data in this plasma discharge for this particular xenon transition.[1] The transition is relatively narrow (approximately 600 MHz) and the velocity and energy distributions in the vicinity of the exit plane is sufficiently broad that the fluorescence trace does not require deconvolution of the transition line shape to produce adequate estimates of the distributions. Not performing the deconvolution further in the plume (e.g. beyond the cathode plane) may introduce uncertainties estimated to be less than 20%. Zeeman splitting is neglected in this analysis due to the broad velocity distributions.

Test Facility

The LIF measurements were performed in Chamber 6 of the Air Force Research Laboratory (AFRL) Electric Propulsion Laboratory at Edwards AFB, CA. Chamber 6 is a non-magnetic stainless steel chamber with a 1.8 m diameter and 3 m length. It has a measured pumping speed of 32,000 l/s on xenon. Pumping is provided by four single stage cryogenic panels (single stage cold heads at 25 K) and one 50 cm two stage cryogenic pump (12 K). Chamber pressure during thruster operation is approximately 1.5×10^{-5} Torr, corrected for xenon.

The thruster is mounted on a three axis orthogonal computer controlled translation system. Figure 1 shows the Hall thruster and optics mounted within the vacuum chamber as well as the LIF apparatus. The laser is a tunable diode laser. It is capable of tuning approximately ±50 GHz about a center wavelength of 834.7 nm. The 6 mW beam is passed through a Faraday isolator to eliminate feedback to the laser. The laser beam then passes through several beam pick-offs until it is focused by a lens and enters the vacuum chamber through a window. The probe beam is chopped at a frequency by an optical chopper (Ch2 at 2.8 kHz) for phase sensitive detection of the fluorescence signal.

The two wedge beam pick-offs (BS) shown in Fig. 1 provide portions of the beam for diagnostic purposes. The first beam pick-off directs a beam to a photodiode detector (D1) used to provide constant power feedback to the laser. The second beam is divided

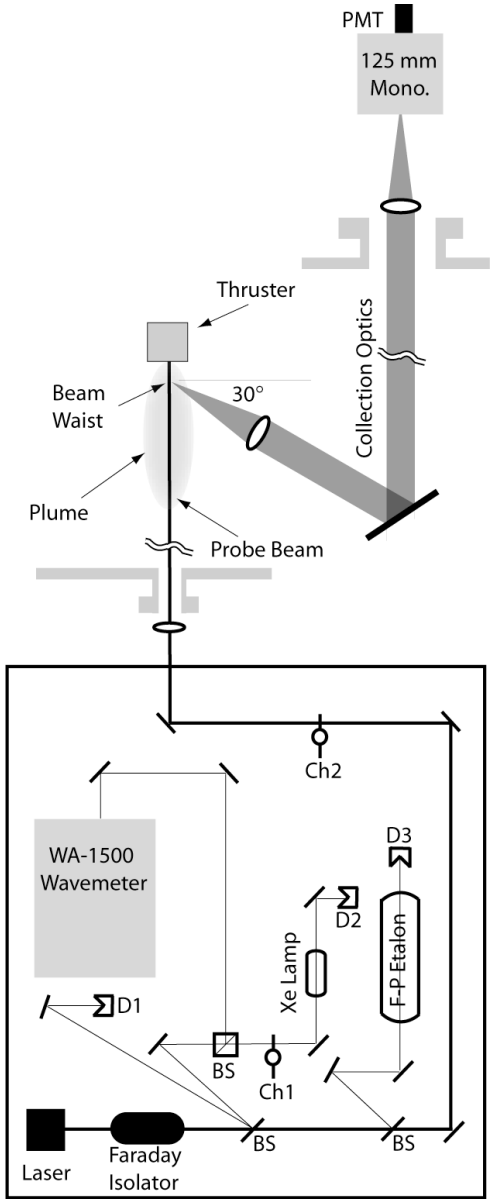

Figure 1. Diagram of the laser optical train and collection optics.

into two equal components by a 50-50 cube beam splitter. The first component is directed to a wavelength meter used to monitor absolute wavelength. The second component is sent through an optical chopper (Ch1 at 1.4 kHz) and through a low pressure xenon hollow cathode discharge lamp. The lamp provides a stationary absorption reference for the determination of the Doppler shift. Unfortunately, there is no detectable population of the ionic xenon $5d[4]_{7/2}$ state. However, there is a nearby (estimated to be 18.1 GHz distant) neutral xenon $6s'[1/2]_1 - 6p'[3/2]_2$ transition at 834.68 nm.[11,12] The second pick-off sends a beam to a 300 MHz free spectral range Fabry-Perot etalon (F-P) that provides high resolution frequency monitoring of the wavelength interval swept during a laser scan.

Table 1. Nominal BHT-HD-600 Hall thruster operating conditions.

Anode Flow	2.453 mg/s
Cathode Flow	197 μg/s
Anode Potential	300 V
Anode Current	2.16 A
Keeper Current	0.5 A
Heater Current	3.0 A

The fluorescence collection optics are also shown in Fig. 1. The fluorescence is collected by a 75 mm diameter, 300 mm focal length lens within the chamber and oriented 60° from the probe beam axis. The collimated fluorescence signal is directed through a window in the chamber side wall to a similar lens that focuses the collected fluorescence onto the entrance slit of the 125 mm focal length monochrometer with a photomultiplier tube (PMT). Due to the 1:1 magnification of the collection optics, the spatial resolution of the measurements is determined by the geometry of the entrance slit 0.7 mm width and 1.5 mm height as well as the sub-mm diameter of the probe beam. This apparatus allows for limited probing of the interior acceleration channel of Hall thrusters with relatively shallow acceleration channels. Measurements show that this combination of apparatus and laser power are well within the linear fluorescence regime.

Hall Effect Thruster

The Hall thruster used in this study is the rectangular 600 W Busek Company BHT-HD-600 Hall thruster with a Busek 3.2 mm hollow cathode. A photograph of the rectangular BHT-HD-600 Hall thruster is shown in Fig. 2. This thruster has a conventional five magnetic core (one inner, four outer) magnetic circuit. The acceleration channel of the thruster has a 32 mm outer radius and a 24 mm inner radius. The acceleration channel has a depth of approximately 10 mm between the geometrical exit plane and the furthest forward extent of the anode. The thruster has been extensively characterized to have a thrust of 39 mN with a specific impulse of 1,530 s yielding an efficiency of approximately 50% at the nominal conditions specified in Table 1.

Figure 3 shows a cut-a-way view of the near field geometry of the Busek BHT-HD-600 Hall thruster. The locations of the central magnetic poles and edges of the acceleration channel are indicated as is the position of the cathode. The Cartesian coordinate system and origin used in these measurements are also shown in Fig. 3, with positive X axis going into the

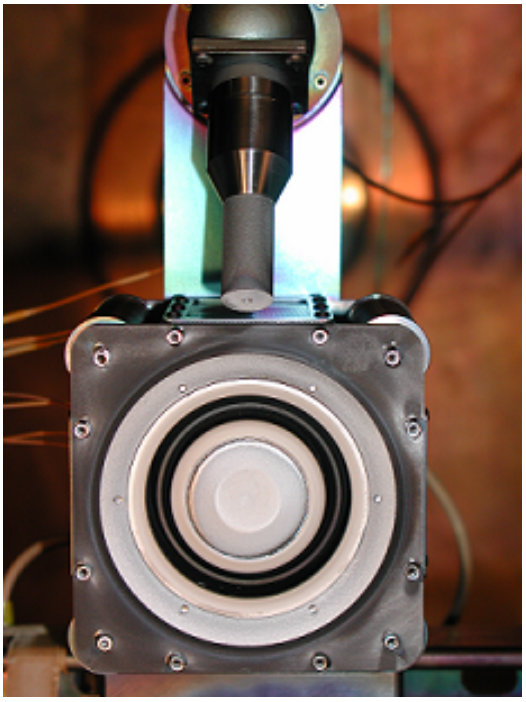

Figure 2. Photograph of the Busek BHT-HD-600 Hall effect thruster.

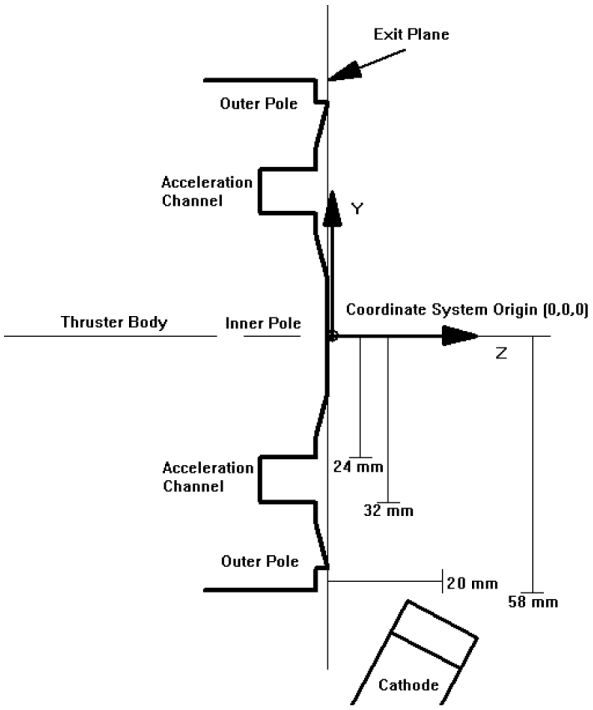

Figure 3. Cross-section of the BHT-HD-600 Hall thruster showing coordinate system of LIF measurements.

page. The origin is at the center of the thruster face due to the ease and repeatability with which this position could be located. All measurements presented in this work will lie on the Z = 0 mm and Z = 28 mm line. This corresponds to the acceleration channel centerline opposite the cathode in the Y-Z plane.

Results and Discussion

Magnetic Field Variation Effects

The magnetic field of the Hall thruster may be varied by changing the applied current to either of the four series connected outer magnetic cores, and, or the central core. In addition to the nominal case, two additional cases are investigated in this effort. These cases represent geometrically similar radial magnetic field profiles with decreases in the magnitude to 85% and 50% relative to the nominal case. Figure 4 shows the calculated shape of the radial magnetic field along the acceleration channel center (Y = 28 mm, X = 0 mm). Although the two off nominal cases are 15% and 50% less in magnitude than nominal, the profiles are geometrically similar. The two off-nominal cases show a maximum -5% deviation from the nominal radial B field, primarily between Z = -4 mm and -8 mm.

In the off-nominal cases, varying the magnetic field does not change the average anode current appreciably. The change from nominal is approximately 2%.

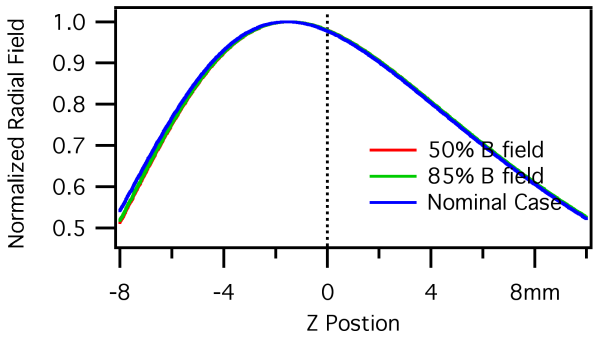

Figure 4. Relative radial magnetic field along the acceleration channel center.

The effect of magnetic field variation on performance has yet to be characterized as thrust measurements for the two off nominal conditions studied in this work are not yet available.

Other measures of the plume such as divergence measurements from Faraday probe measurements show differences, but these are appear to be due to chamber effects as the measurement were taken at either Busek, or AFRL. The largest published set of plume data, by Ekholm, et al, looks extensively at the effect of plume divergence due to variations in anode flow rates and discharge potentials, but does not examine the effect of changes to the magnetic field strength.[13] It is anticipated that a future effort will measure the plume divergence differences of these

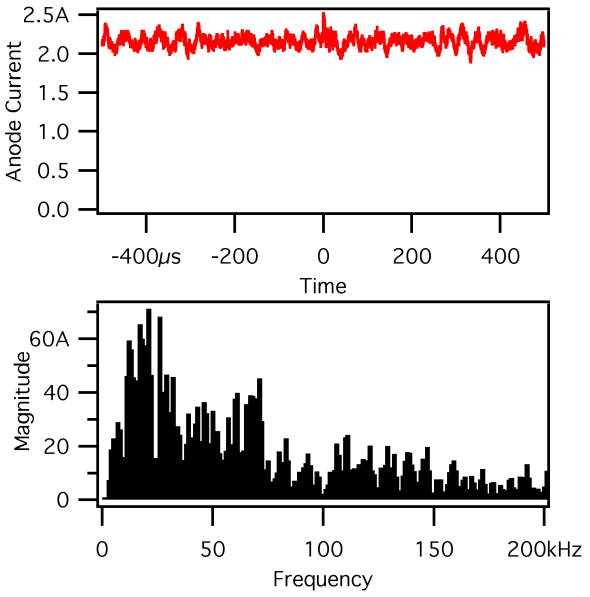

Figure 5. Nominal anode current time and frequency domain behavior.

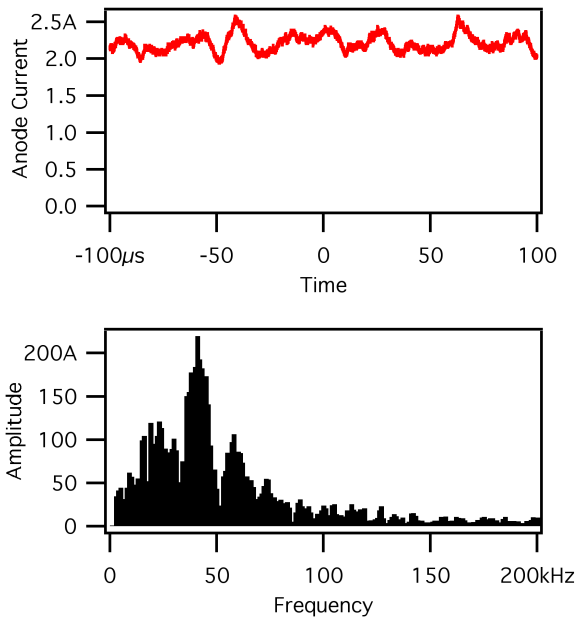

Figure 6. Anode current time and frequency domain behavior for 85% nominal magnetic field case.

three cases.

One effect that is clearly identified and the primary reason for the study of these three particular cases (despite the limited performance and plume data) is the distinct anode current fluctuation behavior of each case. Figure 5 shows the anode current time and frequency domain behavior of the nominal magnetic field case. The anode current is relatively quiescent with a mean of 2.16 A and standard deviation of 77 mA (3.6%).

Reducing the magnetic field by 15% increases the current fluctuations to approximately 5% as shown in Fig. 6. Here the mean anode current is 2.21 A with a standard deviation of 112 mA. These two relatively quiescent cases can be contrasted with the 50% nominal magentic field case in Fig. 7 which has an anode current fluctuation standard deviation of over 34% of the 2.10 A mean. Although the shape of the magnetic field does not change appreciably, the anode current oscillations are strongly influenced. The characteristics of these anode current fluctuations are quantitatively illustrated in the frequency domain plots also shown in Figs. 5, 6, and 7. As the magnitude of the radial magnetic field shown in Fig. 4 decreases, the magnitude of the oscillations increases. Interestingly, as the oscillations increase in magnitude, they also increase in coherence. A single frequency (40 kHz) dominates the 50% magnetic field case, where as the frequencies of oscillation for the nominal case are more broadly dispersed.

It has been hypothesized that the turbulent plasma oscillations in the plasma are responsible for either all or at least a portion of cross field electron diffusion, also commonly referred to as *anomalous electron transport*.[14] There are a number of turbulent modes that could account for the time and frequency domain behavior seen in Figs. 5, 6, and 7.[15,16] These include both azimuthal and axial ionization waves that may in certain cases strongly influence the locations of ion creation and subsequent acceleration within the Hall thruster. This waves are known to occur at frequencies ranging between 10 kHZ and 60 kHz, similar to those shown above.

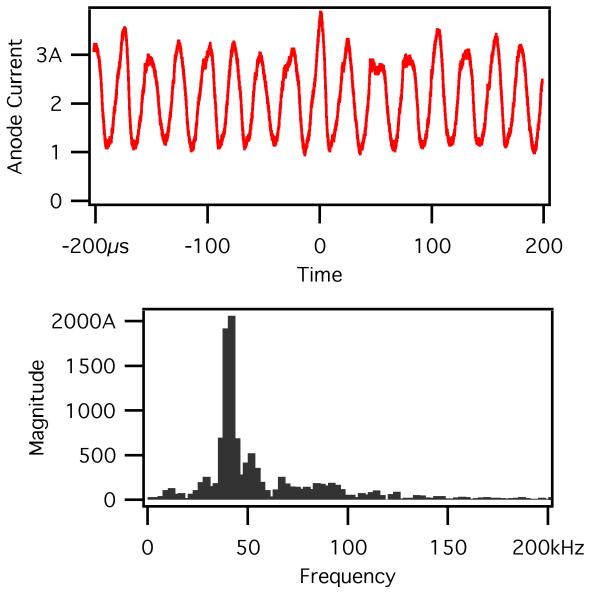

Figure 7. Anode current time and frequency domain behavior 50% nominal magnetic field case..

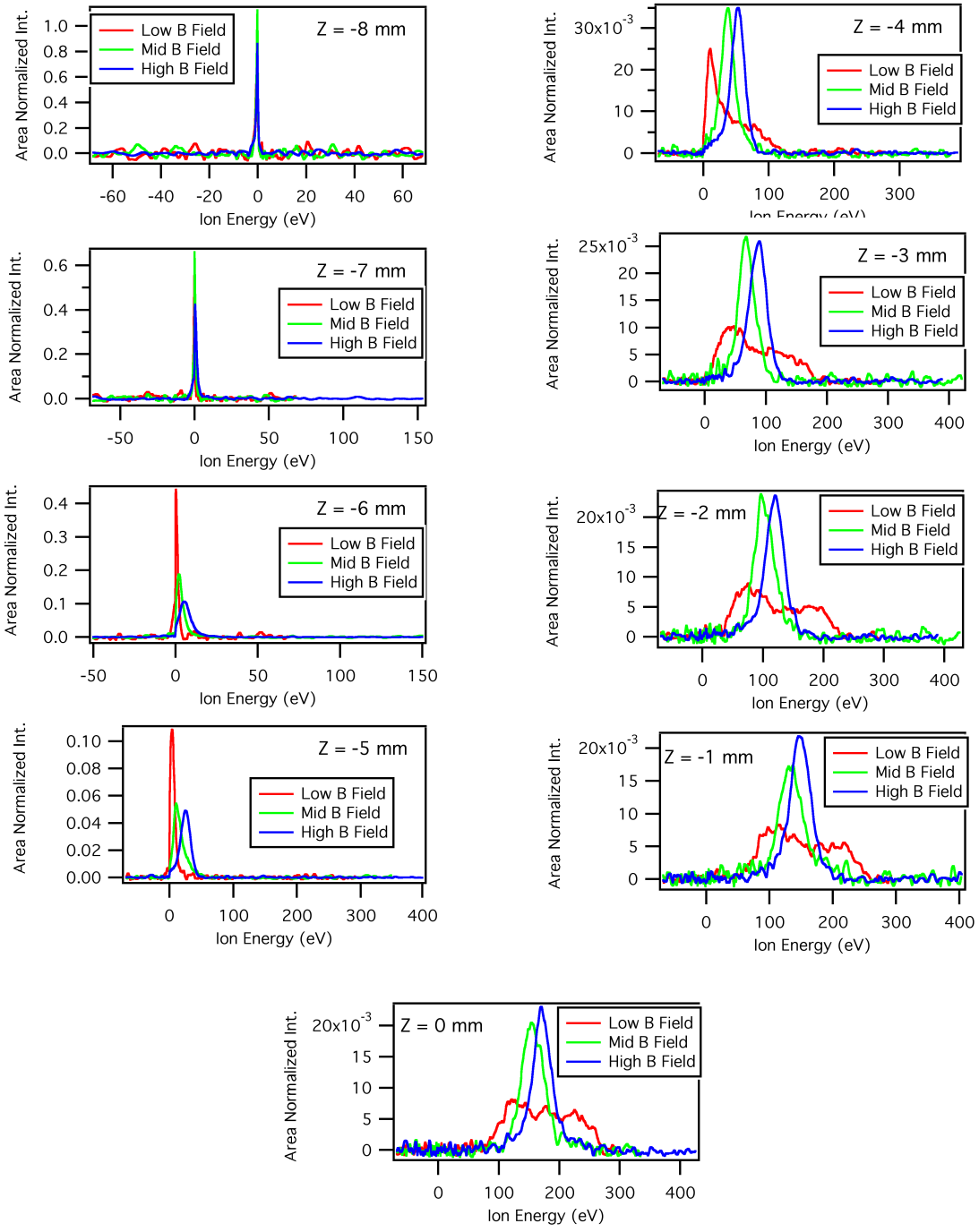

Figure 8. Energy distribution functions between the anode and geometrical thruster exit plane along the acceleration channel centerline.

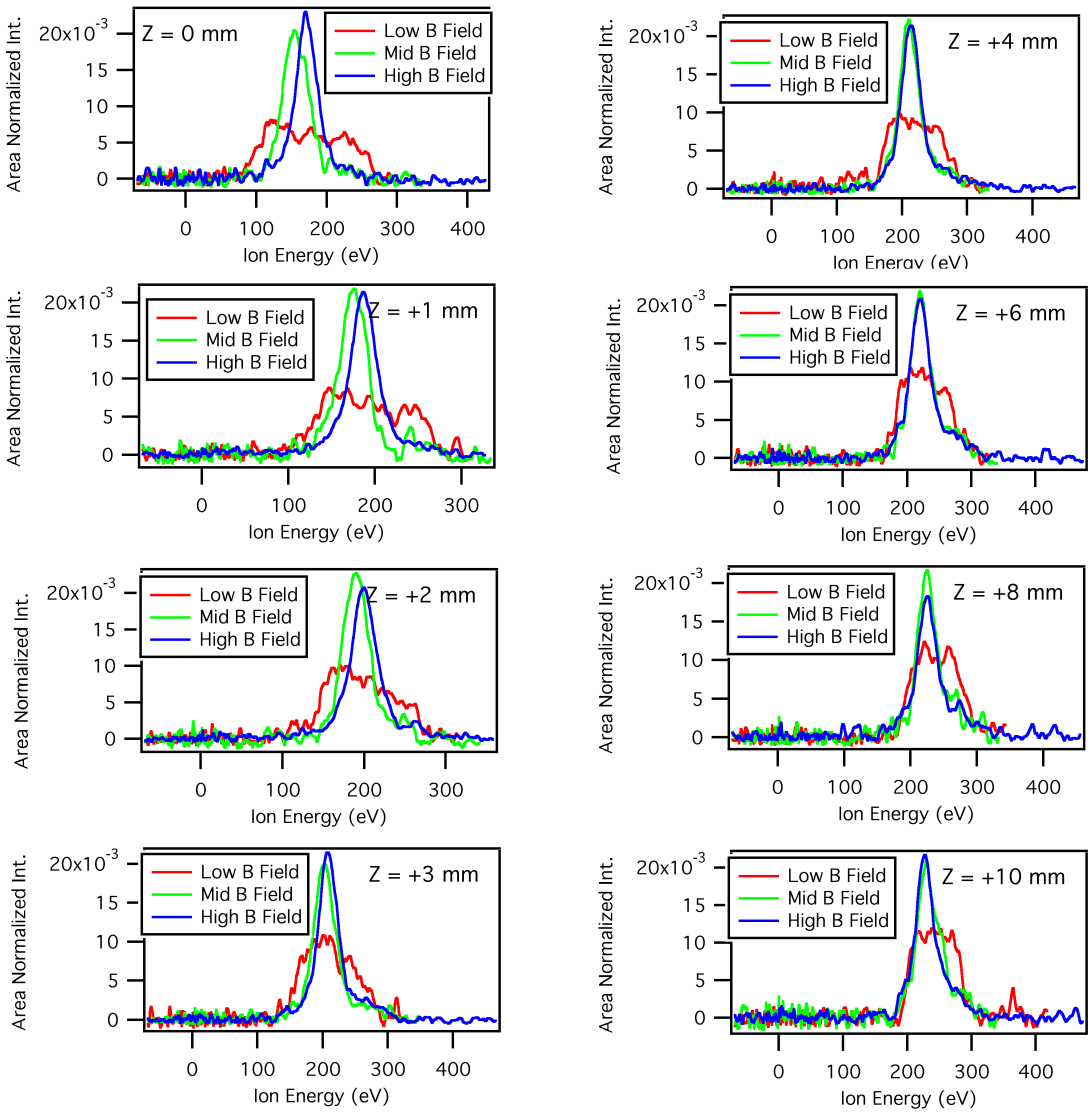

Figure 9. Energy distribution functions outside the geometrical thruster exit plane along the acceleration channel centerline

It is assumed in this work that the oscillations seen in this work are primarily axial and correspond to the so-called *breathing mode*. This assumption appears to be consistent with previous results which have shown the azimuthal wave to dominate at relatively low discharge potentials (less than 200 V) and dissipate at higher values.[16] Since the anode oscillations are in the correct frequency and operating regime, it appears reasonable to consider the oscillations to be indicative of axially traveling ionization and potential waves which strongly influence the local plasma density and conductivity.

LIF Measurements

If the plasma potential and ionization locations are axially traversing portions of the acceleration channel with frequencies on the order of 10's of kHz, the relatively long time averaged velocity distributions (typically 4-7 minutes) will capture approximately of 10^6 of these events. As such, the resulting LIF trace can be used to nonintrusively characterize the severity of the oscillations as well as their physical extent. The three cases for which the oscillatory behavior is characterized in Figs. 5, 6, and 7 represent an ideal test case for LIF investigation of internal Hall thruster oscillations.

Figures 8 and 9 present the energy distribution functions ranging from just above the anode (Z = -8 mm), through the geometrical exit plane (Z = 0 mm), to 10 mm beyond the exit plane (Z = 10 mm). All these measurements were taken at the acceleration channel center (Z = 28 mm) on the X-Y plane (X = 0 mm). Since the plasma oscil-

lations are the result of plasma potential variations, we have chosen to present the LIF data in terms of the ion energy distribution function (EDF). Scaling for all the traces is by area normalization to unity.

In Figs. 8 and 9, the blue traces correspond to the nominal low oscillation case, the green traces correspond to the 80% radial magnetic field strength case, and the red traces correspond to the highly oscillatory 50% radial magnetic field strength case. Examining Figs. 8 and 9, it is immediately obvious that the oscillations have a strong influence on the energy distribution. The nominal case and the 85% nominal magnetic field strength case are are most similar. A portion of the differences in relative peak hight can be attributed to uncertainties arising from the selection of baselines during the normalization procedure due to the noise in the signal. Uniformly, the low magnetic field case (50% nominal) energy distributions are two to three times broader than the nominal and 85% cases. This is particularly pronounced in the interior of the acceleration channel. For example at Z = -3 mm, the energy distribution of the low magnetic field strength case varies between 0 eV and 180 eV. This is approximately 3 times the width of the profiles of the other two higher magnetic field cases.

The energy profiles for each case are shown in Fig. 10. Here for each case we have the median velocity and width of the profile calculated using the full width at half maximum (FWHM) of a Gaussian fit to the EDFs in Figs. 8 and 9. This procedure appears to provide a reasonable and consistent measure of the breadth of the energy distribution and avoids the uncertainties that would otherwise be introduced by calculating the mean and standard deviation of each profile in Figs. 8 and 9. As seen in Fig. 10, the widths of the ion energy distributions are measurably larger for the low magnetic case than the two other more quiescent cases with higher magnetic fields. Interestingly, the highest median velocity at the most downstream location was for the must oscillatory case, by 10 eV and 15 eV relative to the mid and high magnetic field cases. Unfortunately, it is not precisely known which of these cases produces the highest efficiency. Such measurements would determine which of these cases is the most efficient ion accelerator. At present, it is surmised that the more oscillatory cases are less efficient since more high energy ions are created deep within the acceleration channel and are likely to result in more ion recombination due to ion wall impact events.

The widths of the profiles are better compared between the three cases in Fig. 11. The widths of the energy distributions for the nominal and mid range radial magnetic field strength cases are nearly the

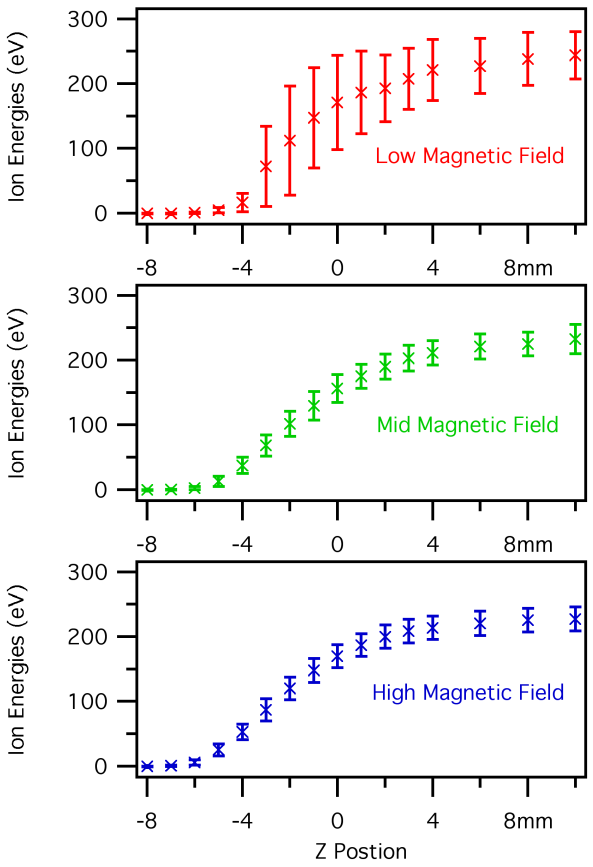

Figure 10. Median ion energies bracketed by ion distribution widths for the three magnetic field cases.

.

same through out the acceleration channel. In both cases, the widths of the ion energy distribution begin near zero and slowly rise reaching a maximum between Z = -2 mm or Z = -1 mm. Downstream, the energy distribution widths of both cases appear to remain constant at approximately 40 eV without appreciable changes.

Meanwhile, the behavior of the low (50% of nominal) radial magnetic field strength case is very different. The energy distribution width follows the other cases until the Z = -4 mm position. Examining Fig. 8, this is the position at which the ions first experience any significant acceleration. A portion of the ions have already been accelerated to as high as 100 eV, and an even larger portion have just been ionized and have less than 30 eV of acceleration. In contrast, the less oscillatory modes appear to have already experienced the majority of their ionization and gained approximately 50 eV of acceleration. Downstream of Z = -4 mm, the low radial magnetic field case has a rapidly growing energy distribution width which grows to a peak of 175 eV at Z = -2 mm, which drops to 100 eV at the exit plane, appears to drop further

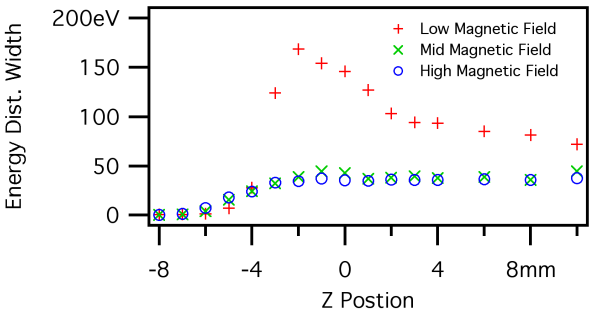

Figure 11. Measured energy distribution widths for the nominal (high), mid, and low radial magnetic field cases.

.

outside the thruster reaching a width of 70 eV at Z = 10 mm.

One possible interpretation for the evolution of the energy distribution of the nominal and 80% radial magnetic field strength cases is that an axial breathing mode oscillation disperses the ion creation region by a potential approaching the measured width of the energy distributions. Alternatively, it is interesting to note that the width of the two more quiescent cases is close to the commonly accepted estimate that the peak electron temperature within the acceleration channel which is approximately one tenth of the discharge potential.

The coherent oscillations of the low radial magnetic field case may manifest as a similarly coherent axial breathing mode ionization wave. It appears to begin at Z = -4 mm rapidly growing and peaking at Z = -2 mm, subsequently decaying in amplitude by Z = 2 mm. In fact at Z = -2 mm, the ion energy distribution of this case strongly suggests two overlapping energy distributions; one centered at 190 eV and another at 70 eV.

There has been some optical evidence that high amplitude oscillations raise the electron temperature significantly in a Hall thruster anode discharge.[17] It appears unlikely that the electron temperature is on the order of the the 170 eV energy distribution width. An increased electron temperature likely only contributes peripherally to the increase to the ion energy distribution width.

Conclusions

This effort has non-intrusively measured xenon ion velocity profiles in the center of the acceleration channel of a medium power (600 W) Hall thruster from the near anode region to 10 mm (0.15 exit diameters) downstream of the geometrical exit. These measurements were taken for three conditions which varied in radial magnetic field strength in a ratio of 1.00 : 0.85 : 0.50. During these tests all other controls (discharge potential, propellent flow rate, background pressure, cathode heater, and cathode keeper current) were unchanged. In the three cases, the anode discharge current varied by only 2%. The primary observed difference between the three cases is the substantial increase in the 10 kHz to 60 kHz anode current breathing mode as the radial magnetic field strength is reduced.

From the ion velocity profiles, ion energy distributions are computed. The case with highest oscillation (and the lowest radial magnetic field strength) has substantially broader ion energy distributions. The LIF diagnostic allows for the nonintrusive characterization of the internal plasma oscillations of this Hall effect thruster.

In this study we have characterized the discharge current oscillations to be breathing mode oscillations generally located at a frequency of 40 kHz. The strength and spectral width of the breathing mode oscillation are linked in the conditions studied and also appear to be inversely dependent on the radial magnetic field strength.

As a result of a strong, coherent breathing mode, the ion energy distributions are up to 4 times broader than when there is a weak, frequency distributed breathing mode. One important consequence of this is that the highly oscillatory case has significant populations of high energy ions much deeper within the Hall thruster than the quiescent cases. The highly oscillatory case also appears to have an extended ionization zone within the thruster acceleration channel. Both these issues are most likely due to a strong and coherent breathing mode axially traveling ionization wave which oscillates within the Hall thruster both distributing the ionization region and dithering the local acceleration potential. It is believed that this two effects best explain the broadened ion energy distributions that result. It is also possible that the relatively high frequency of the breathing mode may result in an elevation of the electron temperature within the Hall thruster acceleration channel. However, it is surmised that any possible electron temperature rise only has a minor effect on the breadth of the ion energy distribution.

Since the strength of discharge current oscillations below 100 kHz has been seen to increase with test chamber background pressure, the results of this work imply that understanding Hall thruster measurements at elevated background pressures is significantly more complex than the simple ingestion of background neutral atoms.[18] It is clear that further investigation of these phenomena are required.

One important aspect of the breathing mode oscillations is their possible effect on Hall thruster life-

time. The lifetime of a Hall thruster is governed by the erosion of the dielectric walls of the acceleration channel. It appears from this work that long term thruster operation in a highly oscillatory regime may reduce thruster lifetime due to the introduction of large populations of high energy ions deep within the acceleration channel combined with a dithering electric field. We are not aware of any study directly linking oscillations to shortened lifetime, but the results of this work support this supposition.

Acknowledgments

The authors would like to thank Mr. Garrett Reed for his assistance in the development of the LIF data acquisition system. In addition, discussions with Dr. Vlad Hruby of the Busek Company were instrumental in the genesis of this paper.

References

[1]W. A. Hargus Jr. and M. R. Nakles, "Evolution of the ion velocity distribution in the near field of the bht-200-x3 hall thruster," in *Proceedings of the 42nd Joint Propulsion Conference and Exhibit*, no. AIAA-2006-4991. American Institute of Aeronautics and Astronautics, July 2006.

[2]W. A. Hargus Jr. and M. A. Cappelli, "Laser-induced fluorescence measurements of velocity within a hall discharge," *Applied Physics B*, vol. 72, no. 8, pp. 961–969, June 2001.

[3]S. Mazouffre, D. Gawron, V. Kulaev, and N. Sadeghi, "A laser spectroscopic study on xe+ ion transport phenomena in a 5 kw-class hall effect thruster," in *Proceedings of the 30th International Electric Propulsion Conference*, no. IEPC-2007-160. Electric Rocket Society, September 2007.

[4]W. A. Hargus Jr. and M. R. Nakles, "Ion velocity measurements within the acceleration channel of low power hall thruster," in *Proceedings of the 30th International Electric Propulsion Conference*, no. IEPC-2007-172. Electric Rocket Society, September 2007.

[5]H. Geisen, T. Krumpelmann, D. Neuschafer, and C. Ottinger, "Hyperfine splitting measurements on the 6265 angstrom and 6507 angstrom lines of seven xe isotopes by lif on a beam of metastable xe(3p0,3) atoms," *Physics Letters A*, vol. 130, no. 4-5, pp. 299–309, July 1988.

[6]W. Fischer, H. Huhnermann, G. Kromer, and H. J. Schafer, "Isotope shifts in the atomic spectrum of xenon and nuclear deformation effects," *Z. Physik*, vol. 270, no. 2, pp. 113–120, January 1974.

[7]L. Bronstrom, A. Kastberg, J. Lidberg, and S. Mannervik, "Hyperfine-structure measurements in xe ii," *Physical Review A*, vol. 53, no. 1, pp. 109–112, January 1996.

[8]D. H. Manzella, "Stationary plasma thruster ion velocity distribution," in *Proceedings of the 30th Joint Propulsion Conference and Exhibit*, no. AIAA-1994-3141. American Institute of Aeronautics and Astronautics, June 1994.

[9]J. E. Hansen and W. Persson, "Revised analysis of singly ionized xenon, xe ii," *Physica Scripta*, no. 4, pp. 602–643, 1987.

[10]W. Demtroder, *Laser Spectroscopy: Basic Concepts and Instrumentation*. Springer-Verlag, 1996.

[11]M. H. Miller and R. A. Roig, "Transition probabilities of xe i and xe ii," *Physical Review A*, vol. 8, no. 1, pp. 480–486, July 1973.

[12]C. E. Moore, *Atomic Energy Levels*. National Bureau of Standards, 1958, vol. II.

[13]J. M. Ekholm, W. A. Hargus Jr., C. W. Larson, M. R. Nakles, G. D. Reed, and C. S. Niemela, "Plume characteristics of the busek 600 w hall thruster," in *Proceedings of the 42nd Joint Propulsion Conference and Exhibit*, no. AIAA-2006-4659. American Institute of Aeronautics and Astronautics, July 2006.

[14]S. Yoshikawa and D. J. Rose, "Anomalous diffusion of a plasma across a magnetic field," *Physics of Fluids*, vol. 5, no. 3, March 1963.

[15]E. Y. Choueiri, "Plasma oscillations in hall thrusters," *Physics of Plasmas*, vol. 8, no. 4, pp. 1411–1426, April 2001.

[16]G. S. Janes and R. S. Lowder, "Anomalous electron and ion accelertaion in a low-density plasma," *Physics of Fluids*, vol. 6, p. 1115, 1966.

[17]W. A. Hargus Jr. and M. A. Cappelli, "Interactions within a cluster of low power hall thrusters," in *Proceedings of the 39th Joint Propulsion Conference and Exhibit*, no. AIAA-2003-5006. American Institute of Aeronautics and Astronautics, July 2003.

[18]R. R. Hofer and A. D. Gallimore, "High specific impulse hall thrusters, part 2: Efficiency analysis," *Journal of Propulsion and Power*, vol. 22, no. 4, pp. 732–740, July-August 2006.